



## IN-PLANE SEISMIC BEHAVIOR OF NEW TYPE MASONRY WALLS WITHOUT JOINT MORTAR

H. Choi<sup>(1)</sup>, KW. Jin<sup>(2)</sup>, JC. Jeong<sup>(3)</sup>, BS. Kim<sup>(4)</sup>, EJ. Hwang<sup>(5)</sup>

<sup>(1)</sup> Associate Professor, Shizuoka Institute of Science and Technology, [choi.ho@sist.ac.jp](mailto:choi.ho@sist.ac.jp)

<sup>(2)</sup> Senior Assistant Professor, Meiji University, [jin@meiji.ac.jp](mailto:jin@meiji.ac.jp)

<sup>(3)</sup> CEO, Nara & Tech Co. Ltd, [illhoco@naver.com](mailto:illhoco@naver.com)

<sup>(4)</sup> Director, Nara & Tech Co. Ltd, [hj44525@hanmail.net](mailto:hj44525@hanmail.net)

<sup>(5)</sup> Senior Researcher, Nara & Tech Co. Ltd, [homeyj@naver.com](mailto:homeyj@naver.com)

### **Abstract**

The authors developed two types of block systems consisting only of main block and key block without joint mortar to improve the seismic performance and to enhance the workability. Two types of block systems have different key block shapes: One is the peanuts shape and the other is the dumbbell shape. In both type blocks, the gap between the main block and the key block is designed to be 1.5 mm on all parts in consideration of workability and manufacturing accuracy. Furthermore, the proposed block systems have a half-height difference between the main block and the key block to be expected high seismic performance in in-plane and out-of-plane directions compared to typical masonry wall with joint mortar.

In this study, in order to evaluate the in-plane seismic performance of the proposed block systems, two types of block walls are experimentally investigated including the typical block wall. In the tests, three full-scale, single-story specimens are tested under in-plane cyclic loading, and failure patterns and cracks are carefully observed.

In this paper, the loading bearing capacity, energy dissipate capacity and reuse ratios of block walls are discussed in detail.

As a result, the deformability, energy absorption capacity and reuse ratio of the proposed block systems were considerably higher than those of typical block system.

*Keywords: unreinforced masonry; in-plane; out-of-plane; main block; key block*



## 1. Introduction

In some regions of Asia, Europe, and Latin America where earthquakes frequently occur, serious earthquake damage is commonly found resulting from catastrophic building collapse. Such damaged buildings often have unreinforced masonry (URM) walls, as shown in Fig.1(a). Since the seismic performance of the URM wall buildings and infill walls are relatively poor compared to the other structural types, these buildings and walls always damaged when an earthquake occurs. Furthermore, in Japan which is an earthquake-prone country, the use of URM walls is prohibited by the Building Standards, but concrete block fences with reinforcing bars are often used. However, the damage of the fences always occurred when the earthquake occurs, as shown in Fig.1(b).

Under these backgrounds, the authors developed two types of block systems consisting only of main block and key block without joint mortar in consideration of seismic performance and workability. Two types of block systems have different key block shapes: One is the peanuts shape and the other is the dumbbell shape.

In this study, the proposed two types of concrete block walls as well as a typical concrete block wall were experimentally investigated to evaluate the seismic performance. In the tests, full-scale, single-story specimens were tested under static cyclic in-plane loading, and failure patterns and cracks were carefully observed.

In this paper, the loading bearing capacity, energy dissipation capacity and reuse ratio of block walls are discussed in detail.



(a) L'Aquila earthquake, Italy (2009)



(b) Northern Osaka earthquake, Japan 2018

Fig. 1 – Masonry wall damage

## 2. Outline of Experiment

### 2.1 Proposed block systems

The authors developed two types of concrete blocks to improve the seismic performance of both in- and out-of-plane directions and to enhance the workability without the joint mortar [1]. The two types of concrete blocks only consist of main blocks and key blocks, and they have different key block shapes: One is the peanuts shape and the other is the dumbbell shape, as shown in Fig.2.

As shown Fig.2, the gap between the main block and the key block was designed to be 1.5mm on all sides in consideration of workability and manufacturing accuracy. As can be found in Fig.3, the proposed block systems have half-height difference between the main block and the key block. Therefore, the seismic



performances in the out-of-plane direction as well as the in-plane direction of the proposed block systems are expected to be much higher than that of typical masonry walls.

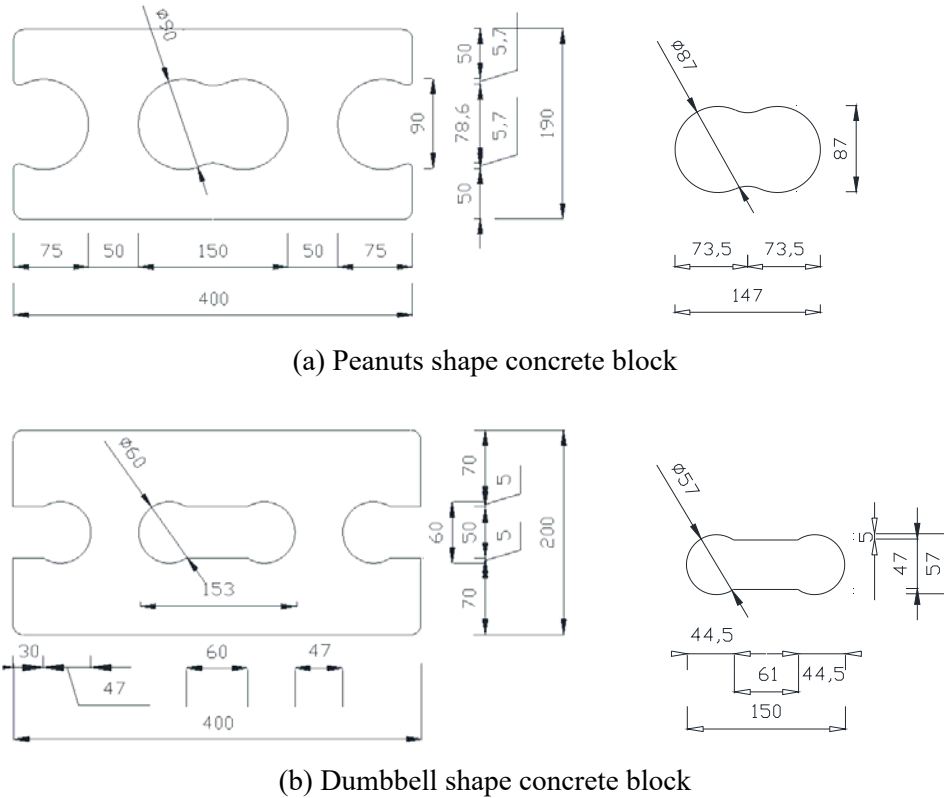


Fig. 2 – Two types of concrete block systems (unit: mm)

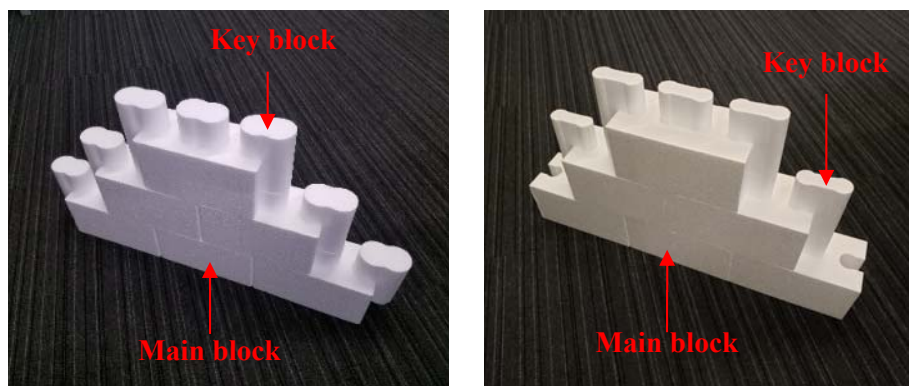


Fig. 3 – Construction of the proposed block walls

## 2.2 Material characteristic

Each concrete block material test results are shown in Table 1 (the average values of three samples are shown in the table). The typical concrete block and peanut shape concrete block were made by the normal cement-to-sand ratio of 1:3.5 used in Korea. Since the dumbbell shape concrete block was, however, used higher cement ratio, the compressive strength is the highest value among three concrete blocks, as shown in



Table 1. The compressive strength of the peanut shape concrete block is higher than that of the typical concrete block, because the peanut shape concrete block has the key blocks in hollow parts of the main block.

Table 1 – Mechanical properties of each concrete block

	Compressive strength (N/mm <sup>2</sup> ) <sup>1)</sup>		
	Typical concrete block	Peanut shape concrete block <sup>2)</sup>	Dumbbell shape concrete block <sup>2)</sup>
Block unit	8.8	14.9	22.0
Block prism <sup>3)</sup>	5.8	7.7	18.1

1) to whole area 2) with key blocks 3) 3-layered specimen

### 2.3 Test specimens

In this study, three full-scale, single-story specimens were designed and fabricated supposing the single-story storage building, as shown in Fig.4: (a) typical concrete block wall specimen with joint mortar (Specimen CB); (b) seismic block wall with peanuts shape key block without joint mortar (Specimen PS); (c) seismic block wall with dumbbell shape key block without joint mortar (Specimen DS). The specimen size is 2.0 m by 1.4 m, as shown in Fig.4.

The typical concrete block wall can resist only friction force to the horizontal load after losing the adhesive force between concrete block and joint mortar. On the other hand, the proposed concrete block wall systems are expected higher deformability due to the shear key mechanism between the main block and the key block.

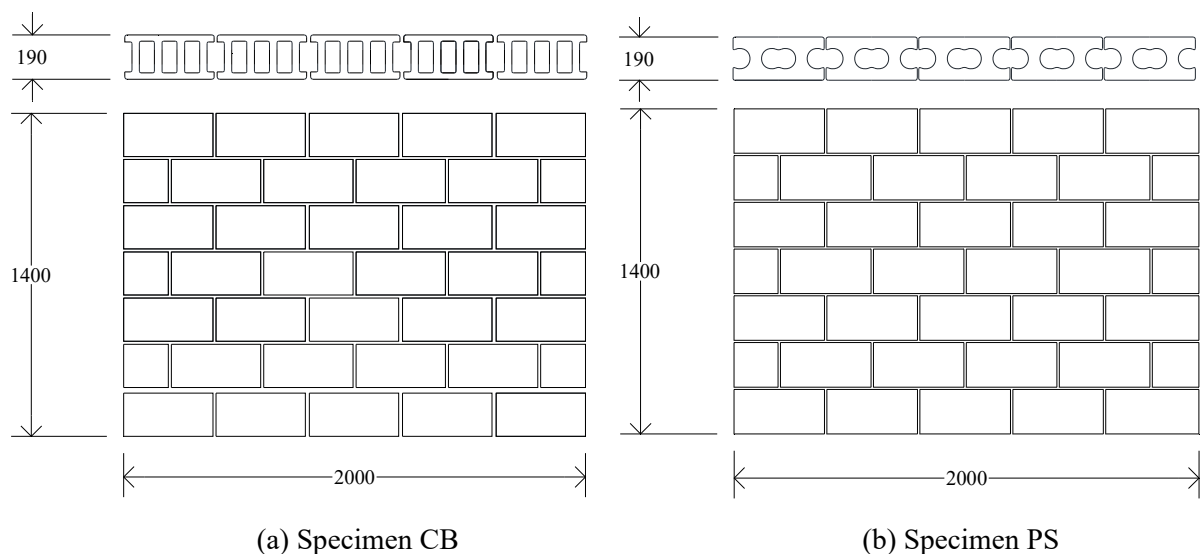


Fig. 4 – Details of typical and proposed concrete block wall specimens (unit: mm)

### 2.4 Test program

A loading system for the static cyclic in-plane tests is shown in Fig.5. Lateral loads in the positive and negative directions were applied to the left end of the upper beam with hydraulic actuators. As mentioned above, since the reference building of this study is a single-story storage building, the axial load was considered as the weight of the upper beam (13.7 kN, axial stress,  $\sigma_0=0.04$  N/mm<sup>2</sup>). Fig.6 shows a lateral loading protocol that was controlled by a drift angle  $R$ , defined as a lateral drift  $\Delta$  at the top-center of specimen divided by the height from the bottom of the specimen,  $H$ , as shown in Fig.5.



The measurement system is shown in Fig.7. The relative lateral displacement, the lateral displacement at each layer of wall, the vertical displacement of both ends of specimen, and diagonal deformation of wall were measured, respectively. Furthermore, the maximum crack widths at peak loads and residual crack widths at unloaded stages were carefully measured.

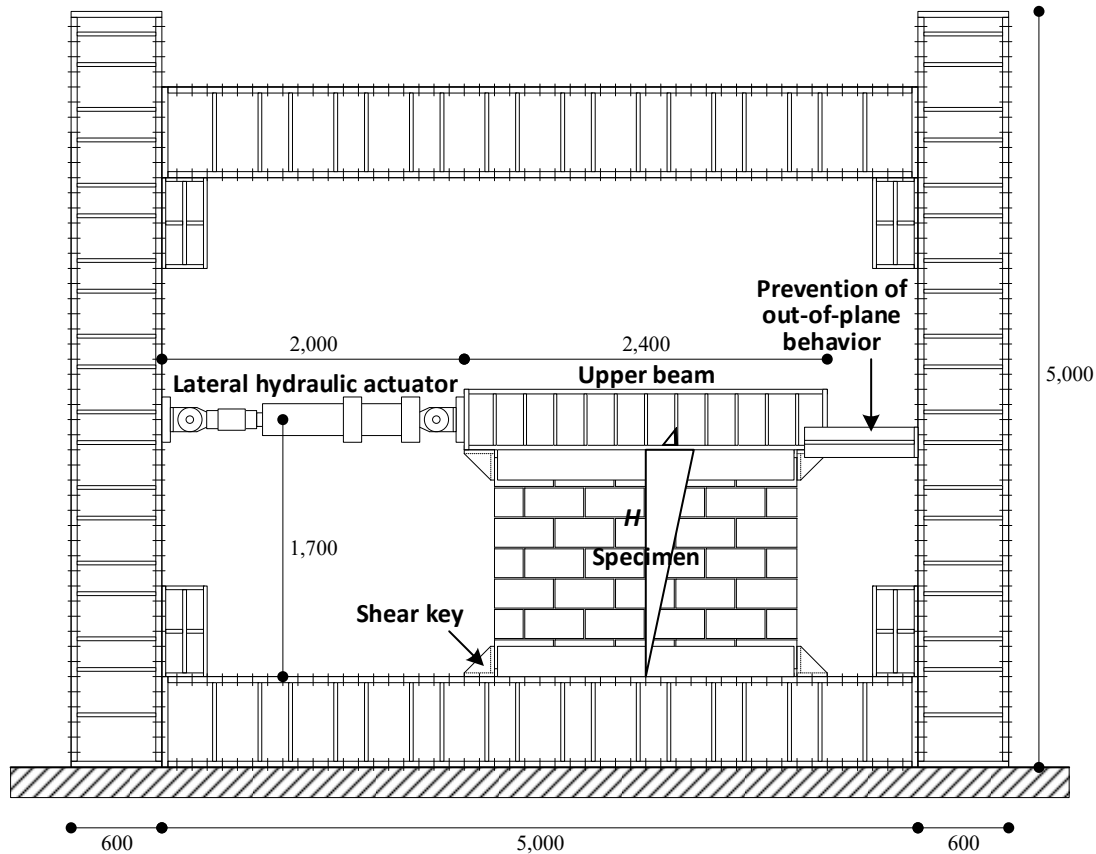


Fig. 5 – Loading system (unit: mm)

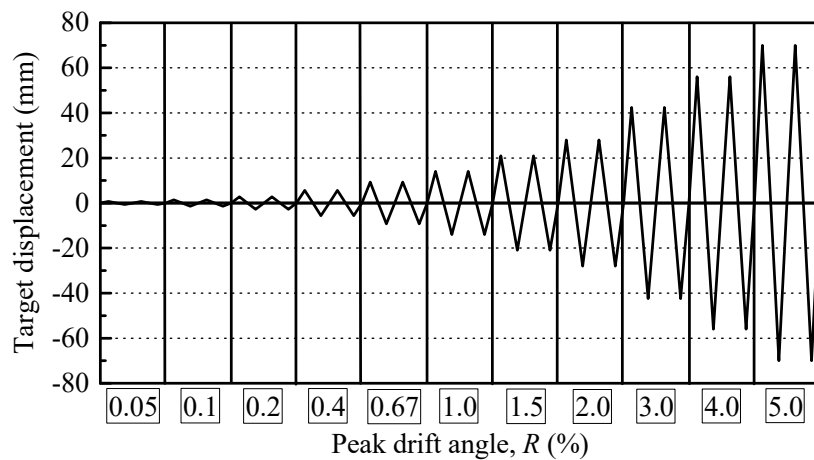


Fig. 6 – Lateral loading protocol

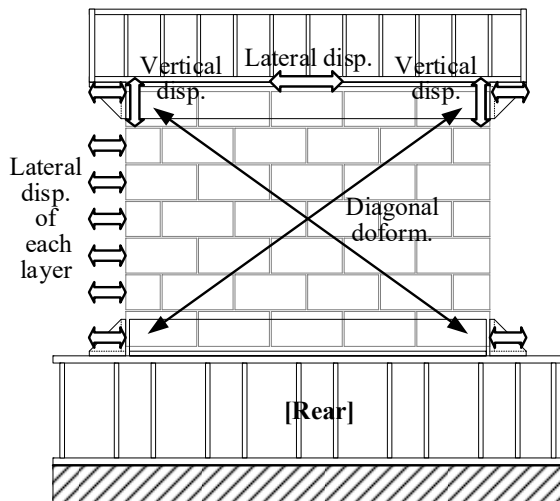


Fig. 7 – Measurement system

### 3. Experimental Results

#### 3.1 Failure patterns and lateral force – drift angle relationships

Fig.8 and Fig.9 show the damage patterns after final loading and the lateral force–drift angle relationships of all specimens, respectively. The behavior of each specimen to failure is summarized below.

##### 3.1.1 Specimen CB

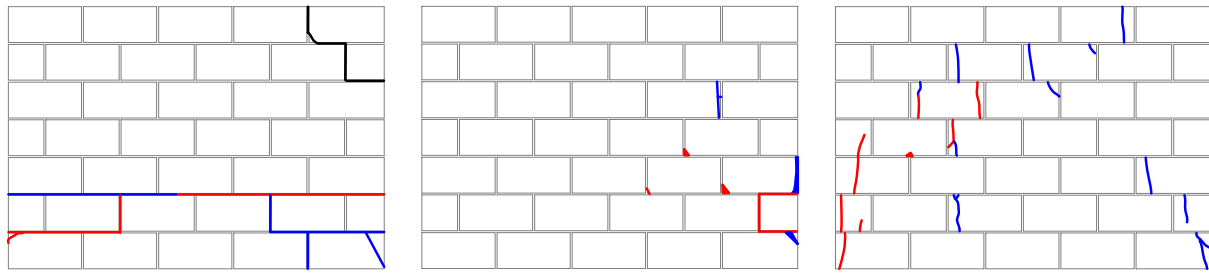
During the first loading drift,  $R$ , of 0.05% rad., the cracks were observed in the entire bed joint (horizontal joint) causing slippage between second and third joint interface. Since the shear crack in the bottom of compression side was occurred during  $R = 0.67\%$  rad., the test was terminated at  $R = 1.0\%$  rad. Until the final loading, this specimen showed the rocking behavior between second and third layers. The maximum strength of 14.7 kN was recorded at  $R = 0.67\%$  rad. and no remarkable strength deterioration is found until  $R = 1.0\%$  rad.

##### 3.1.2 Specimen PS

The small width crack was occurred on the main block of the right-bottom end at  $R = 0.25\%$  rad. This specimen also showed the rocking behavior until final loading because of low axial force according to the single-story storage building. Since the crushing and spalling off of the main block where is the rightmost side of the second layer was occurred at  $R = 5.0\%$ , the experiment was terminated after  $R = 5.0\%$ . The maximum strength of -17.5 kN was recorded at  $R = -2.0\%$  rad. and no remarkable strength deterioration is found until the final loading.

##### 3.1.3 Specimen DS

This specimen has more vertical cracks on the main blocks than Specimen PS. The small width cracks were occurred on the main blocks of the both bottom ends at  $R = 0.1\%$  rad. This specimen also showed the rocking behavior. Since the crushing and spalling off of the main block where is the both ends of the second layer was occurred at  $R = 5.0\%$ , the experiment was terminated after  $R = 5.0\%$ . The maximum strength of 19.7 kN was recorded at  $R = 3.0\%$  rad. and no remarkable strength deterioration is found until the final loading.



(a) Specimen CB

(b) Specimen PS

(c) Specimen DS

Fig. 8 – Final crack patterns (Blue: Positive dir., Red: Negative dir., Black: Initial cracks)

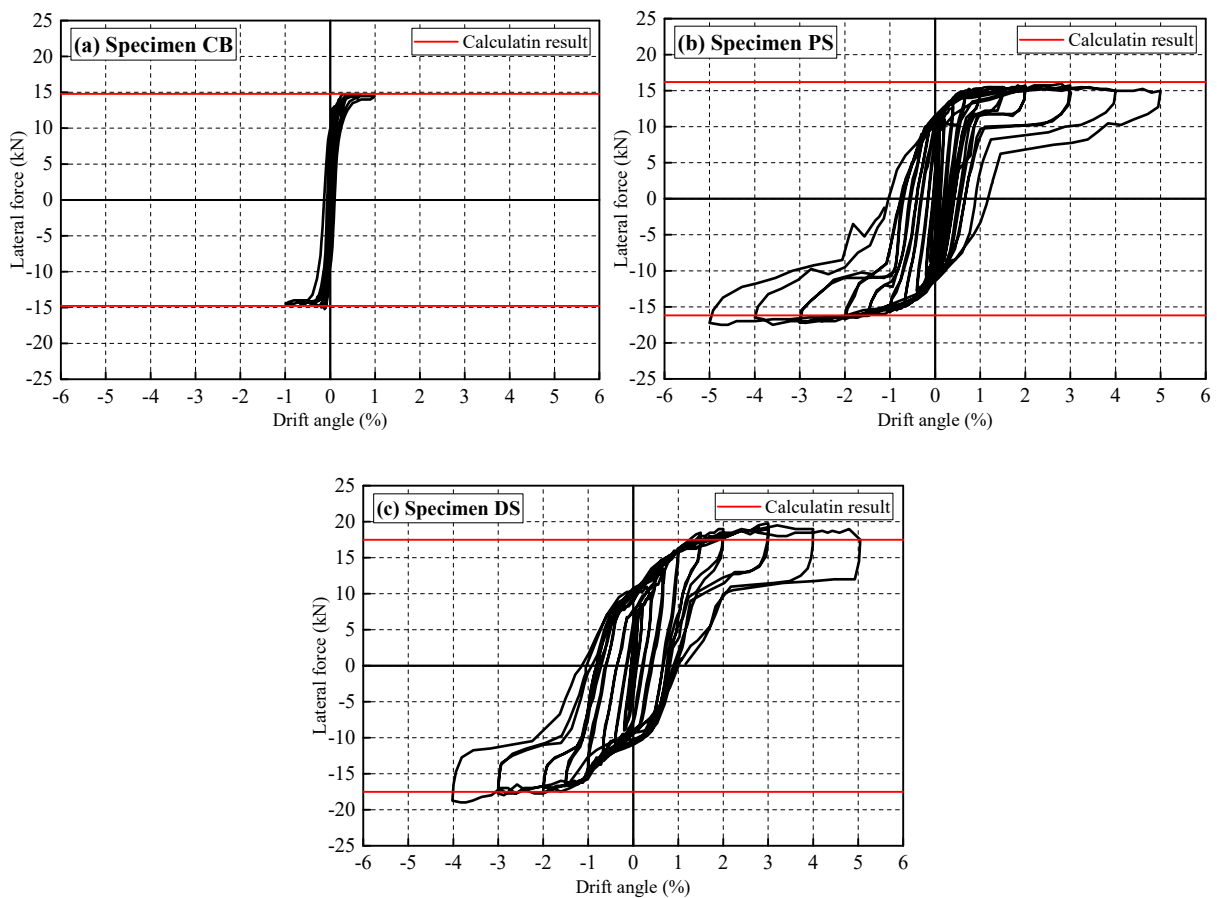


Fig. 9 – Lateral force – drift angle relationships of each specimen

### 3.2 Comparison of in-plane seismic performance of each specimen

#### 3.2.1 Lateral force – drift angle relationships

Fig.10 shows the skeleton curves of each specimen. As shown in the figure, the in-plane seismic performances of Specimens PS and DS were much higher than that of Specimen CB. In particular, the deformability of the proposed system has improved remarkably due to the shear key mechanism between the main blocks and the key blocks.

In this study, the additional simple monotonic loading tests were carried out for verifying the rocking behavior, as shown in Fig.11. 3-layered specimens with typical, peanuts shape and dumbbell shape blocks, respectively, were used in the tests. As shown in Fig.12, the axial loads were considered as the sum of the



weight of the upper loading beam ( $N_1 = 3.7$  kN) and the self-weight of the specimen ( $N_2 = 0.4$  kN, 0.6 kN and 0.72 kN of typical, peanuts and dumbbell shape 3-layered specimens, respectively). The calculated lateral loads were shown in Fig.13 with the test results. As can be found in the figure, the calculated lateral loads agreed well with the experimental results. Among the test results, the increased lateral force of the typical block specimen may result from the adhesive force by the joint mortar.

The lateral loads of Specimens CB, PS and DS were calculated based on the same manner, as mentioned above. Fig.14 shows the rocking mechanism of Specimens CB, PS and DS. As can be found in the figure, the axial loads were considered as the sum of the weight of the upper beam ( $N_1 = 13.7$  kN) and the self-weight of the specimen ( $N_2 = 6.0$  kN, 9.0 kN and 10.8 kN of Specimens CB, PS, DS, respectively). The calculated lateral loads were shown in Fig.9. As shown in figure, the calculated lateral loads show good agreement with the experimental results.

### 3.2.2 Equivalent viscous damping ratios

In order to compare the energy dissipation capacities of all specimens, the equivalent viscous damping ratios were calculated, as shown in Fig.15. The results of the proposed systems considerably had higher values than that of Specimen CB. Furthermore, the remarkable deterioration of the ratios of the proposed systems were not found until the final loading.

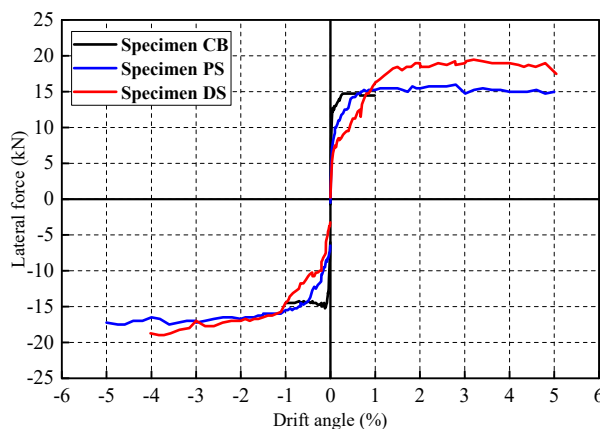


Fig. 10 – Skeleton curves of each specimen

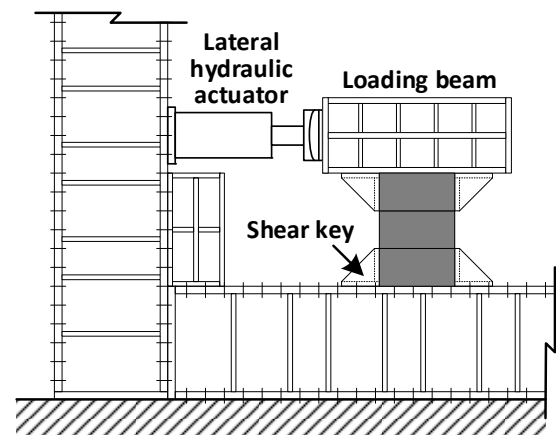


Fig. 11 – Loading system for verifying rocking behavior

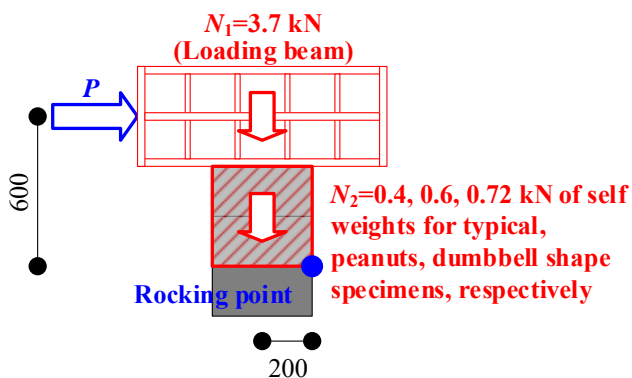


Fig. 12 – Lateral load  $P$  due to rocking behavior

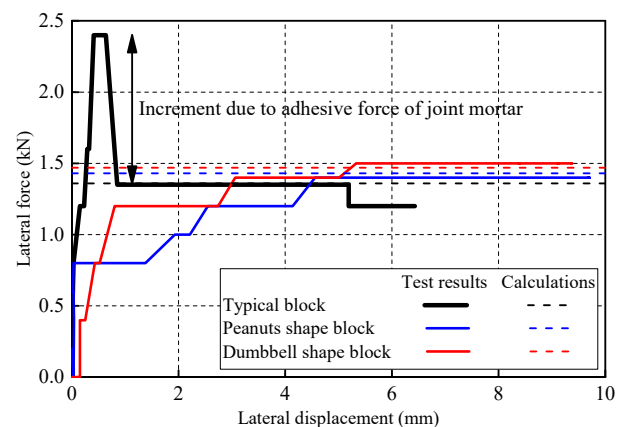
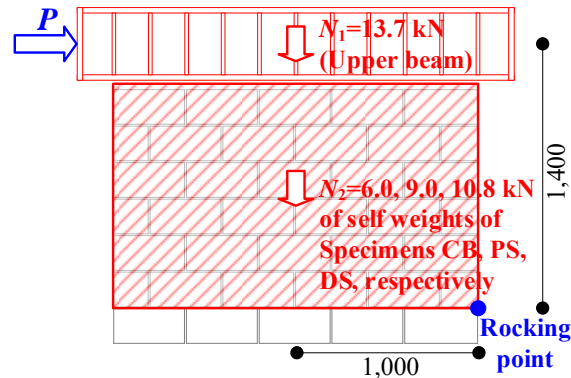


Fig. 13 – Monotonic loading tests vs. calculation results



Fig. 14 – Lateral load  $P$  due to rocking mechanism

### 3.2.3 Reuse ratios of Specimens PS and DS

The typical concrete block and brick may not commonly reuse because of the using of the joint mortar. On the other hand, the proposed systems consisted of only main and key blocks without joint mortar can reuse. In this study, the reuse ratio is defined as the ratio of no damage main blocks to all main blocks. Fig.16 shows the reuse ratio of Specimens PS and DS. As can be found in the figure, the proposed seismic block systems can reuse more than 70% after  $R = 5.0\%$  rad. This result imply that the proposed concrete block wall systems are economical and eco-friendly.

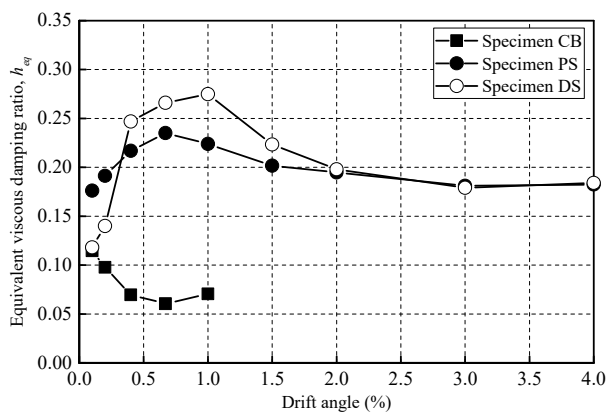


Fig. 15 – Equivalent viscous damping ratios

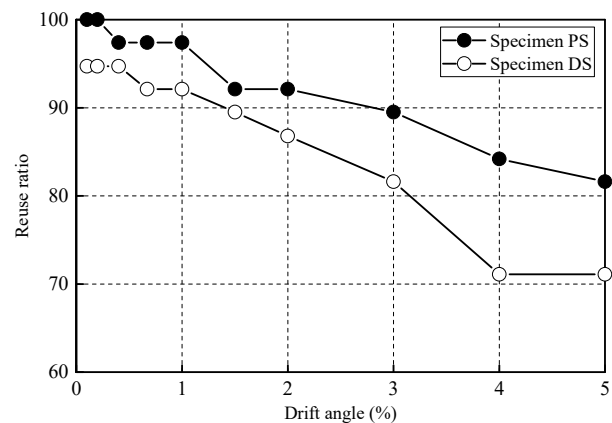


Fig. 16 – Reuse ratios of the main blocks

## 4. Conclusions

The current paper presented the experimental tests of the two types of new concrete block walls as well as a typical block wall and investigated the in-plane behaviour, the loading bearing capacity, energy dissipation capacity and reuse ratio. The following major findings were obtained:

- [1] The in-plane seismic performances of Specimens PS and DS were much higher than that of Specimen CB. In particular, the deformability of the proposed system has improved remarkably due to the shear key mechanism between the main blocks and the key blocks.
- [2] The calculated lateral loads based on the simple rocking mechanism agreed well with the experimental results.



- [3] The energy dissipation capacities of the proposed systems considerably had higher values than that of Specimen CB. Furthermore, the remarkable deterioration of the ratios of the proposed systems were not found until the final loading.
- [4] The proposed seismic block systems can reuse more than 70% after final loading. This result imply that the proposed concrete block wall systems are economical and eco-friendly.

The current paper focused only on the in-plane experimental behavior. The experimental data should be investigated from numerical perspectives, and the out-of-plane experimental and numerical behaviours should be carried out, in future studies.

### **Acknowledgements**

The project was funded by the JSPS Grant-in-Aid for Scientific Research (Category (c), Grant No. 18K04425, Principal Investigator: Ho Choi) and the Joint Research with Nara & Tech Co. Ltd. The authors are thankful to both agency and company for their financial support.

### **References**

- [1] Choi H, Jin KW, Jeong JC, Kim BS, Hwang EJ and Jin C, 2019, Feasibility Study on Seismic Block without Joint Mortar, Part1 Shape Determination using Finite Element Analysis, Summaries of Technical Papers of Annual Meeting, Architectural Institute of Japan, Vol.4, 2019.9, pp.977-978